EFFECT OF INTERFACE DEFECT STATES ON PHOTOELECTRIC PROPERTIES OF $In_xGa_{1-x}As/GaAs$ HETEROSTRUCTURES WITH QUANTUM DOTS

O.V. VAKULENKO,[1] S.L. GOLOVYNSKYI,[1] S.V. KONDRATENKO,[1] YU.I. MAZUR,[2] ZH.M. WANG,[2] G.J. SALAMO[2]

[1]Taras Shevchenko National University of Kyiv, Faculty of Physics
(64, Volodymyrs'ka Str., Kyiv 01601, Ukraine; e-mail: golovinskiy.serg@gmail.com)

[2]Arkansas Institute of Nanoscale Materials Science and Engineering, University of Arkansas
(Fayetteville, AR 72701, USA)

PACS 71.20.Nr;72.20.Pa

Properties of the lateral photocurrent in $In_xGa_{1-x}As/GaAs$ heterostructures with quantum dot (QD) chains at various indium concentrations x are investigated. At the interband excitation of QDs by quanta with $h\nu = 1.2$ eV, the structures have revealed a long-term rise and the relaxation kinetics of the photocurrent as well as the effect of residual conductivity after the exciting radiation is turned off. Analyzing the data on thermostimulated conduction (TSC) after the excitation by optical radiation in the region of QD absorption, the following energy levels of defect states with respect to the GaAs conduction band were found: 0.11 eV, 0.16 eV, 0.21 eV, 0.24 eV, and 0.35 eV. Investigations of the lateral photoconduction (LPC) made it possible to discover transitions involving the levels of electron traps of $EL2$ and $EB3$ GaAs intrinsic defects. In the simplest case of a nanostructured photoconductor with one trapping center, we obtained an analytical expression for the photocurrent kinetics of conduction electrons that was confirmed by experiments with $In_{0.4}Ga_{0.6}As/GaAs$ samples. The kinetics of $In_{0.5}Ga_{0.5}As/GaAs$ photoconductors is more complex and described only qualitatively.

1. Introduction

Heterostructures with self-organized quantum dots attract attention from the viewpoint of fundamental physics and their practical application in optoelectronics. The electron structure and the optical properties of such systems are determined by the QD shape and size, their composition profile, mechanical stress distribution, and so on [1]. $In_xGa_{1-x}As$ QDs surrounded by GaAs belong to structures, in which the motion of charge carriers of both signs (electrons in the conduction band and holes in the valence band) is somewhat restricted. These structures are particularly characterized by interband and intraband transitions with the participation of quantum-sized states successfully used in infrared photodetectors, light-emitting diodes, and lasers [2, 3].

Investigations of photoelectric properties of two-dimensional heterostructures based on $A_{II}B_{VI}$ and $A_{III}B_V$ compounds, silicon, and so on, have revealed a complex conduction mechanism. These structures manifest the long-term relaxation kinetics of the photocurrent and the effect of residual conductivity resulting in the registration of thermally stimulated current bands [4, 5]. Such defects are caused in general by structural defects that can spatially separate charge carriers due to their localization at defect trapping centers. $In_xGa_{1-x}As/GaAs$ heterostructures with QDs are not an exclusion. The mismatching of the lattice constants of $In_xGa_{1-x}As$ QDs and their GaAs surrounding ($\sim 7\%$) results in considerable mechanical stresses in the QD vicinity, which causes, in turn, the formation of interface defects. The latter can significantly influence the properties of systems with QDs and, thus, the operation of electronic and optoelectronic devices on their basis.

One of the effective methods in deep-level spectroscopy of crystal and amorphous semiconductors is thermostimulated conduction (TSC) [6–8]. In contrast to the standard and more widespread Deep-Level Transient Spectroscopy (DLTS), the TSC method is preferable when analyzing traps in low-conductivity heterostructures, where charge carriers are transferred along barrier layers.

In this work, we analyze the effect of deep levels on the conductivity and the photoconductivity of heterostructures with $In_xGa_{1-x}As$ QDs at various relative concentrations of In/Ga. It is shown that, at temperatures of < 200 K, the deep levels in a QD vicinity accumulate the negative charge, which causes the residual conductivity and TSC. The photoelectric properties of samples with

 ISSN 2071-0194. Ukr. J. Phys. 2011. Vol. 56, No. 9

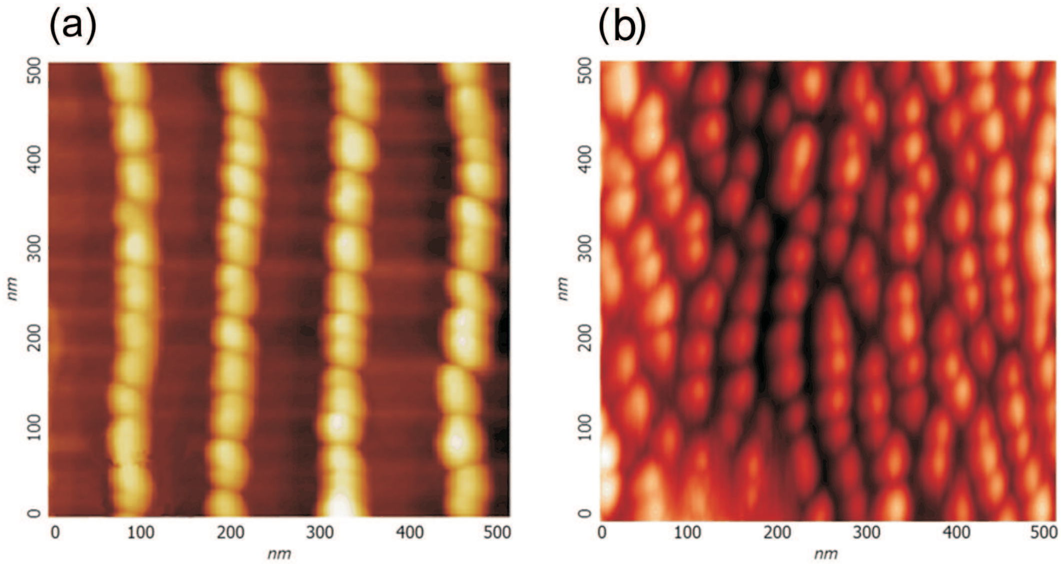

Fig. 1. AFM images of the upper layer of the $In_{0.4}Ga_{0.6}As/GaAs$ (a) and $In_{0.5}Ga_{0.5}As/GaAs$ (b) heterostructures

different In concentrations (and thus different amounts of defects in the structure) are compared.

2. Experiment

The multilayer $In_xGa_{1-x}As/GaAs$ heterostructures under study were grown by the molecular beam epitaxy technique on a semiinsulating GaAs substrate with (100) crystal orientation of the cut surface. After removing an oxide layer from the surface, a buffer 0.5-nm thick GaAs layer was grown on it at the temperature $T_S = 600$ °C. After that, the substrate temperature was reduced to 540 °C, and N periods of $In_xGa_{1-x}As/GaAs$ were grown. The nominal indium concentration x in two types of the studied multilayer $In_xGa_{1-x}As/GaAs$ structures was equal 0.4 or 0.5. The growth rate of GaAs and $In_xGa_{1-x}As$ amounted to 0.4 and 0.8 ML/s, respectively. The sample was grown at a constant pressure of As vapors equal to 1×10^{-5} Torr. The transition from the pseudomorphic two-dimensional (2D) growth mode to the formation of nanoislands was controlled, by observing the diffraction of high-energy electrons. The structures were grown so that QDs had a chain-like arrangement. The sample surface morphology was studied with the help of a scanning atomic force microscope Ntegra (NT-MDT) (Fig. 1). The data on the surface density ρ, average width w, and height h of QDs obtained in this way are collected in Table 1.

T a b l e 1. Parameters of $In_xGa_{1-x}As/GaAs$ heterostructures with QDs

x	N	ρ, μm^{-2}	w, nm	h, nm	DC (77 K), A
0.4	7	200	40	5	$0,6 \times 10^{-8}$
0.5	17	290	40	5	$< 10^{-11}$

As one can see from Table 1, samples with a larger In content are characterized by the much smaller conductivity. To our mind, it is due to the increase of the difference between the lattice constants of $In_{0.5}Ga_{0.5}As$ and GaAs in the heterotransition region as compared to the system with $x = 0.4$. Thus, in the case of $In_{0.5}Ga_{0.5}As/GaAs$, it is worth expecting larger mechanical stresses in the interface and antistructural defects with attributes of $EL2$ electron traps – with levels close to the middle of the forbidden band, which provides a high resistivity of the given material. A result (or a proving argument) of the higher defectness of the structure with $x = 0.5$ is a lower space order in QD chains, whereas a consequence of larger mechanical stresses in this structure can be a higher QD density (Fig. 1).

To study the longitudinal photocurrent, dark current, and TSC, rectangular contacts 1×6 mm^2 in size based on the Au-Ge eutectic alloy were formed on the sample surface with epitaxial layers at a distance of 5 mm from each other and alloyed into all epitaxial layers (inset in Fig. 2,b). The LPC spectral dependences were measured using an infrared spectrometer in the photon energy range from 0.2 eV to 1.6 eV under normal incidence of the exciting radiation. The voltage applied to the sample was $U = 16$ V. The dark current and the photocurrent were registered in the temperature range

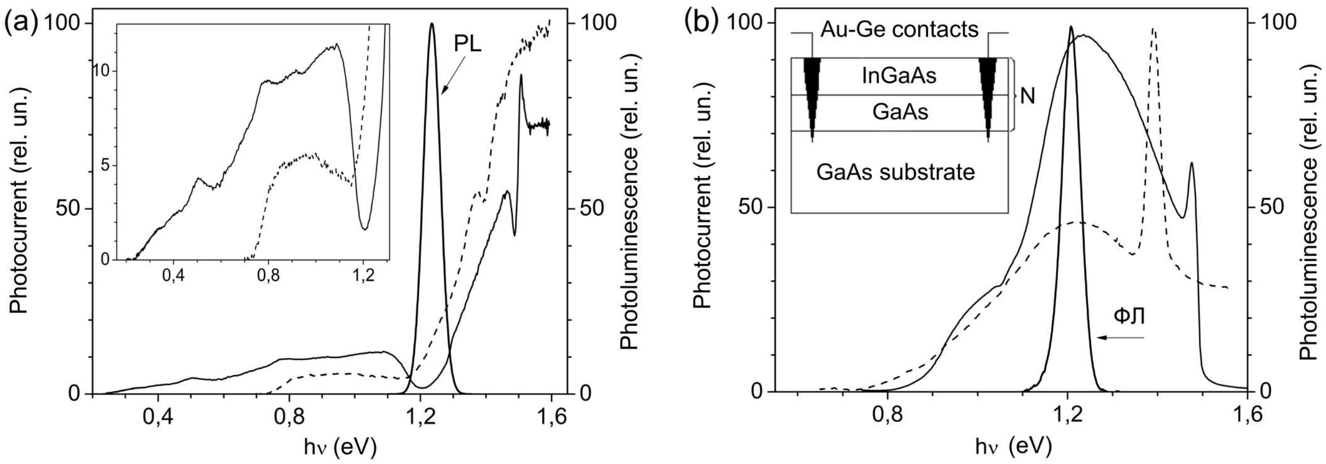

Fig. 2. LPC spectra at 77 K (solid curve) and 290 K (dotted curve) and PL spectra at 77 K (thick solid curve) for the $In_{0.4}Ga_{0.6}As$/GaAs (*a*) and $In_{0.5}Ga_{0.5}As$/GaAs (*b*) structures. In the inset -– structure of the studied samples with $In_xGa_{1-x}As$ QDs and the geometry of eutectic Ge–Au contacts

from 77 to 290 K with the use of a current amplifier and a standard equipment to register the constant photocurrent. The photoluminescence (PL) spectra were measured according to the standard technique using an infrared spectrometer in the energy interval 0.8–1.6 eV under excitation by a laser with a wavelength of 404 nm and a power density of 5 W/cm^2. The spectral width of the gap in this range of measurements amounted to 17 meV. The sample temperature was 77 K, and a cooled Ge photoreceiver was used as a detector.

The rise and relaxation kinetics of the photocurrent were investigated at 77 K. The samples were excited with monochromatic light with the photon energy $h\nu = 1.23$ eV during the time interval t_E. After the excitation is turned off, we registered the relaxation kinetics of the photocurrent until it reached a plateau. To measure TSC, a sample was first cooled to a temperature of 77 K, then illuminated during the time t_E, kept in darkness for 5 min, and after that heated at a constant velocity of 0.16 °C/s.

3. Results and Discussion

3.1. Photoconduction and photoluminescence spectra

Different locations of the Fermi level in the studied structures result in different shapes of the LPC spectrum in the infrared region, because electrons from filled levels can be activated by optical excitation and contribute to the photocurrent.

In the spectral region, where crystal GaAs is transparent ($h\nu < 1.43$ eV at 290 K and $h\nu < 1.51$ eV at 77 K), nonequilibrium charge carriers are generated due to optical transitions involving QD states, deep interface levels, and defect GaAs.

The number and the arrangement of levels in a quantum well change depending on the dimensions of InGaAs QDs and the In content. According to the performed calculations, the studied structures had one quantizing level for electrons in the QD conduction band (E_{e1}) and two quantizing levels for heavy holes in the QD valence band (E_{hh1} and E_{hh2}). The energy of transitions involving ground and excited QD states observed for LPC spectra amounts to $h\nu$ 1.20–1.46 eV at 77 K and 1.14–1.36 eV at room temperature for the structure with $x = 0.4$ (Fig. 2,*a*) and 1.07–1.46 eV at 77 K and 1.00–1.35 eV at room temperature for the structure with $x = 0.5$ (Fig. 2,*b*). In this region, the form of the photoconduction spectrum reflects, first of all, qualitatively the features of the optical absorption spectrum of QDs with various sizes, which is confirmed by the nonuniform widening of the PL bands [9].

For $h\nu$ lower than the energy of interband transitions, a component of the photocurrent of different nature was observed in QDs, namely transitions involving deep levels. Depending on their filling in the equilibrium state, different types of electron transitions are possible. For the $In_{0.4}Ga_{0.6}As$ structure with one trapping level, the minimal quantum energy resulting in the photocurrent amounted to 0.24 ± 0.01 eV at 77 K and 0.74 ± 0.01 eV at room temperature (Fig. 2,*a*). Thus, the optical ion-

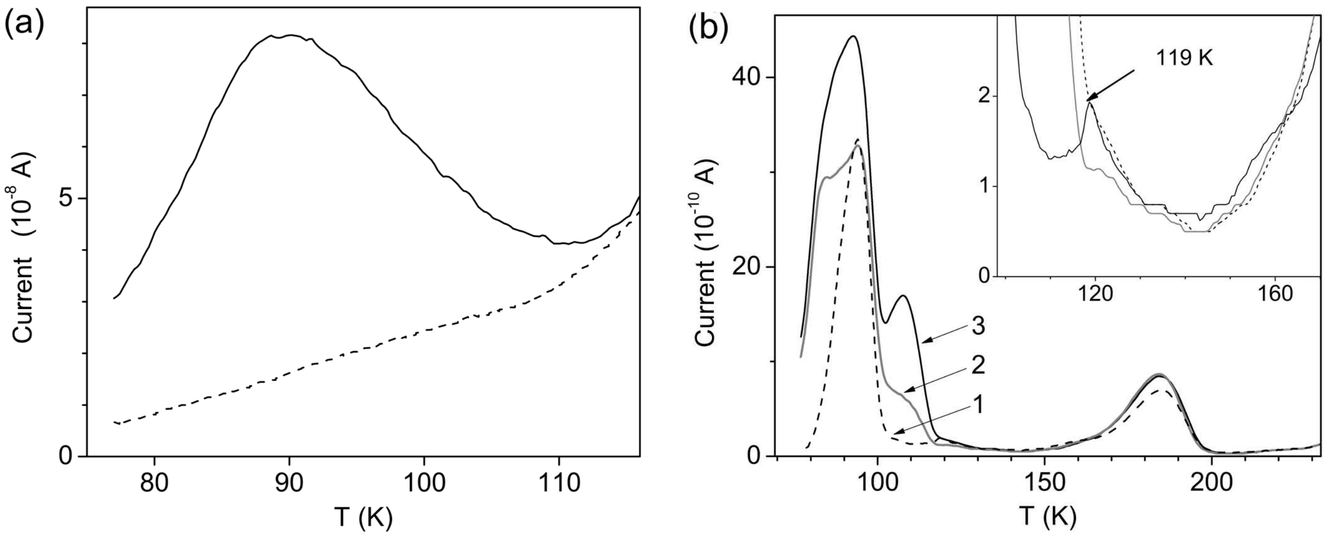

Fig. 3. Temperature dependences of TSC (solid curve) and dark current (dotted curve) of the $In_{0.4}Ga_{0.6}As/GaAs$ structure (*a*) and TSC of the $In_{0.5}Ga_{0.5}As/GaAs$ structure after various times of excitation (*1* – t_E = 350 s, *2* – t_E = 650 s, *3* – t_E = 900 s) (*b*)

ization energy of a defect, that localizes electrons at $T = 77$ K, is equal to 0.24 eV.

Judging by data on the energy spectrum of intrinsic defects in GaAs at the InGaAs/GaAs interface, the photocurrent of the $In_{0.4}Ga_{0.6}As/GaAs$ structure in the regions $h\nu \geq 0.58$ eV at 77 K and $h\nu \geq 0.74$ eV at 290 K is related to electron traps belonging to the $EL2$ family (0.6 eV and 0.75–0.85 eV) and $EB3$ family (0.9 eV) studied by the DLTS technique in [10–13]. In the LFC spectra of the structure with $x = 0.5$ in the region $h\nu < 0.74$ eV (Fig. 2,*b*), there is no photocurrent caused by electron transitions from energy levels of electron traps less deep than $EL2$ (0.75–0.85 eV).

3.2. Temperature dependence of thermostimulated conduction

The energy level spectrum of charge carriers in $In_xGa_{1-x}As/GaAs$ heterostructures with QDs in the temperature range between 77 and 290 K (Table 2) was obtained from TSC investigations. Figure 3 shows TSC graphs of the structures excited by light quanta with the energy $h\nu = 1.23$ eV during various time intervals t_E and subsequently kept in darkness.

The number of the observed TSC peaks depended on the location of the Fermi level. In structures with a larger amount of electron traps $In_{0.5}Ga_{0.5}As/GaAs$ with states located close to the middle of the forbidden band, the Fermi level is located lower, which allows one to observe a wider spectrum of deep levels with the help of the TSC method.

In Fig. 3,*a*, one can see the TSC graph of the $In_{0.4}Ga_{0.6}As/GaAs$ structure. The TSC peak with a maximum close to T_m 88 K testifies to the presence of a deep electron state localized in intermediate GaAs layers near QDs. With regard for the absence of retrapping (capture by other trapping centers), the activation energy of the low-temperature peak can be correctly determined if analyzing the slope of the initial region of the rise curve based on the expression [8, 14]

$$I_{\rm TSC} \sim \exp\left(-\frac{E_c - E_t}{k_{\rm B}T}\right). \qquad (1)$$

Here, E_t stands for the energy position of the trapping center ($\varepsilon_t = E_c - E_t$ is the activation energy of an electron from a trap to the GaAs conduction band), and $k_{\rm B}$ is the Boltzmann constant. The analysis of the curve yields the thermal activation energy of conduction $\varepsilon_t^{\rm B} = 0.165 \pm 0.01$ eV. The obtained value of activation energy agrees with DLTS studies that have revealed an electron trap in InAs/GaAs structures with QDs. This trap is caused by defects near a QD, and its depth relative to the GaAs conduction band is equal to 160 meV. The electron trapping cross section $\sigma_n = 9 \times 10^{-16}$ cm^2 [10].

Unlike the structure with $x = 0.4$, where only one state with $\varepsilon_t^{\rm B} = 0.165$ eV was empty under equilibrium conditions, the time of keeping a sample in light for the $In_{0.5}Ga_{0.5}As/GaAs$ structure considerably influenced the general form of TSC curves, though had no effect on the positions of separate maxima (see Fig. 3,*b*). This fact testifies to the complex process of charging of local trapping centers, as well as to their different nature. After the completion of photoexcitation ($t_E = 350$ s), one registers the least number of peaks at the very beginning of the kinetic dependence. Thus, the centers charged in the first place are impurity centers with maxima of TSC peaks close to 91 K and 187 K. This can be due to their larger electron trapping cross section, as well as to peculiarities of a spatial localization of these levels. In the case of several trapping centers, there exists the retrapping between them, that is why the activation energy can be correctly determined from expression (1) only for the low-temperature peak. Using Eq.(1) and analyzing the initial region of the curve with a peak close to 91 K, one can determine the depth of the level with respect of the conduction band: $\varepsilon_t^{\rm B} = 0.16 \pm 0.01$ eV. This value coincides with that obtained for a trap in the $In_{0.4}Ga_{0.6}As/GaAs$ structure, which testifies to the same nature of this localization level for the both samples.

A longer photoexcitation ($t_E = 650$ s) results in the widening of the low-temperature slope of the curve T_m 91 K due to the charging of a less deep localization level. Because of the close energy positions of two levels, we could not resolve their TSC curves. Analyzing the initial region by the previous method, one still can estimate the thermal activation energy of conduction of this level $\varepsilon_t^{\rm A} = 0.11 \pm 0.01$ eV.

After the photoexcitation with $t_E > 900$ s, at which a plateau is observed at the kinetic curve (Fig. 2,*b*), there appears an additional TSC maximum close to 107 K. With regard for the above explanation of the nature of the "burst" and its relaxation, a conclusion can be made that the TSC peak with $T_m = 107$ K is related to electron traps remote from QDs and other traps located in their vicinity. The energy depth of this level $\varepsilon_t^{\rm C}$ with respect to the conduction band can be approximately estimated using the expression [8]

$$\varepsilon_t = 23 k_{\rm B} T_m, \qquad (2)$$

where T_m is the temperature of the maximum of the TSC peak. This formula yields the following estimate: $\varepsilon_t^C = 0.21 \pm 0.02$ eV.

In view of the fact that the optical ionization energy practically always exceeds the thermal one, one can conclude that it was the electron trap with E_c – 0.21 eV that made a contribution to the photocurrent in the $In_{0.4}Ga_{0.4}As/GaAs$ heterostructure starting from 0.24 eV. For the $In_{0.4}Ga_{0.6}As/GaAs$ structure, this trapping level was not registered by the TSC method, which confirms the fact that this energy level is filled in the equilibrium state, i.e. the Fermi level in the heterostructure lies above the level of this electron trap.

For all TSC curves of the $In_{0.5}Ga_{0.5}As/GaAs$ structure, we registered a peak close to T_m 187 K, whose form remained invariable under various conditions of the experiment. Substituting the position of the maximum into (2), one can find the depth of this electron localization level: 0.35 ± 0.02 eV. The obtained value of the activation energy agrees with DLTS studies of InAs/GaAs structures with QDs, that have revealed an electron trap with the 0.35-eV depth relative to the GaAs conduction band referred to *EL*6 traps in GaAs [10].

It is also worth noting the presence of a weak peak with T_m 119 K shown in the inset of Fig. 3,*b*. Using expression (2), one can estimate the depth of this localization level: $\varepsilon_t^D = 0.24 \pm 0.02$ eV. Such a depth corresponds to the *EB*2 trap discovered in $Al_{0.33}Ga_{0.67}As/GaAs$ structures of *n*-type [15] grown on a semiinsulating GaAs (311) substrate. It is associated with the *E*4 defect of complex nature that includes vacancies of type III (interstitial or antistructured $As_{\rm III}$) and arsenide vacancies (interstitial element of group III or $III_{\rm As}$).

3.3. Photocurrent kinetics

The time step of the photocurrent of the $In_xGa_{1-x}As/GaAs$ heterostructures with QDs excited with $h\nu = 1.235$ eV from the beginning of photoexcitation to saturation has revealed a long-term rise kinetics at 77 K (Fig. 4). The energy of exciting light quanta corresponded to the maximum of the PL band (Fig. 2), i.e. the interband transition involving the ground states of the conduction band and the QD valence band. At this excitation energy, one also observed a photoconduction component caused by the interband excitation of QDs (Fig. 2). For the $In_{0.4}Ga_{0.6}As/GaAs$ structure, one first registers the relatively fast kinetics of the signal, at which the photocurrent considerably grows, after which it rises much slower and reaches a plateau (Fig. 4,*a*). In the case of photoexcitation of the $In_{0.5}Ga_{0.5}As/GaAs$ structure, the photocurrent does not immediately increase: first, it grows rather slowly, then sharply rises, which is followed by an abrupt fall and the transition to a plateau (Fig. 4,*b*).

Electrons and holes generated due to interband transitions in QDs are localized in QDs and cannot participate in charge transfer processes. These carriers can make

T a b l e 2. Results of the analysis of TSC curves

Parameters	trap A	trap B	trap C	trap D	trap E
Peak, T_m	~ 80 K	~ 90 K	~ 107 K	~ 119 K	~ 187 K
$E_c - E_t$	0.11 eV	0.16 eV	0,21 eV	0.24 eV	0.35 eV

 ISSN 2071-0194. Ukr. J. Phys. 2011. Vol. 56, No. 9

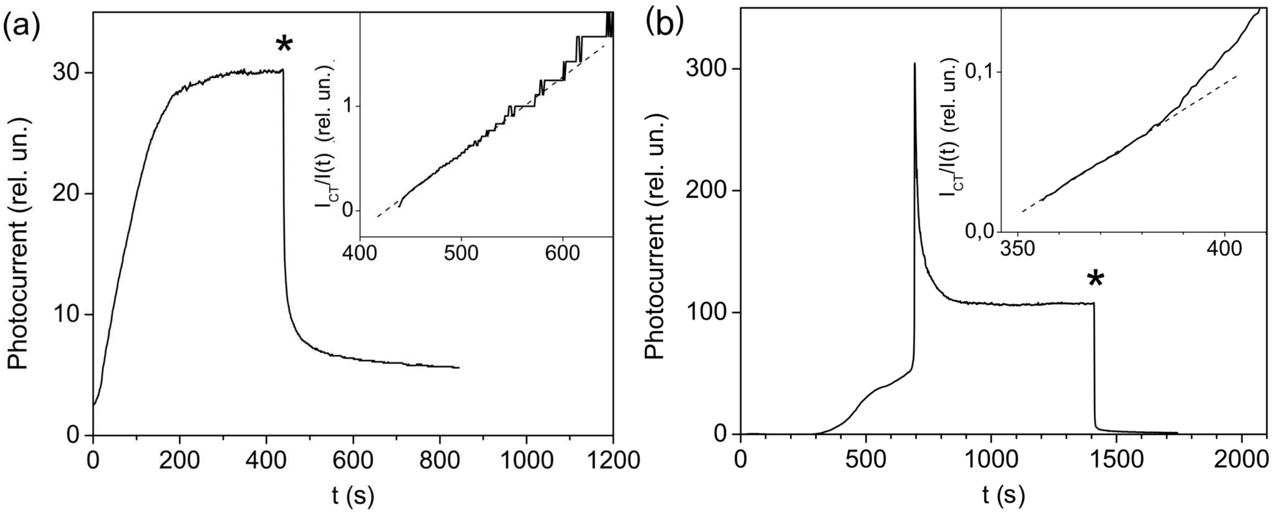

Fig. 4. Rise and relaxation kinetics of the photocurrent of the $In_{0.4}Ga_{0.6}As/GaAs$ (a) and $In_{0.5}Ga_{0.5}As/GaAs$ (b) structures at 77 K. The star marks the moment, at which excitation is turned off. Insets present dependences of I_{st}/I on t

a contribution to the photocurrent if excited electron-hole pairs appear spatially separated, for example due to the thermofield electron transition to intermediate GaAs layers and/or WL. Transitions of such a kind are considered as spatially indirect, similarly to tunnel transitions under the conditions of the Franz–Keldysh effect or transitions at the thermofield ionization of impurities (Poole–Frenkel effect). Works [16–18] are particularly devoted to the study of the effect of processes of thermal emission on the transverse transport and the photoluminescence in $In_xGa_{1-x}As/GaAs$ heterostructures. It is shown that the thermal emission dominantly occurs into GaAs states and/or WL, whereas the channels of radiationless recombination of electron-hole pairs are mainly presented by interface states and dislocations at QD, WL, and GaAs interfaces.

In the both heterostructures, the photocurrent did not completely relax during the observation time after the completion of the photoexcitation (Fig. 4). One can assume the following model of "frozen" photoconduction. Spatially indirect electron transitions result in the filling of trapping centers and cause an increase of the dark (nonequilibrium) conduction. Trapping centers can be local levels of the surrounding of QDs unoccupied at this temperature. Local levels can be formed in the close surrounding of QDs due to dislocations and other lattice defects at the interface of QDs with WL or GaAs (QD interface) [11, 19–21].

Thus, the phenomenon of residual conductivity can be explained by the residual spatial separation of nonequilibrium charge carriers between the QD levels localizing holes and the trapping centers in the QD surrounding localizing electrons. Electrons localized at levels of interface states participate in the conduction due to their thermal transition to the conduction band of intermediate GaAs layers and/or WL. In the case of existence of several electron traps in the interface, the photoexcitaion process can be accompanied not only by spatial separation of charges of an electron-hole pair but also by the optical recharging of electron traps [22, 23].

The theory of photoconduction kinetics in the simplest case of one trapping level is as follows.

Light absorption in a quantum medium (or QD) takes place at the quantum energies $h\nu \geq \varepsilon_L$, where ε_L is the width of the QD forbidden band. In the process of absorption, electron-hole pairs — excitons -– are generated. After that, they either recombine (mainly with radiation in a spectral band with the maximum $h\nu \approx \varepsilon_L$) or dissociate due to the tunneling of an electron of the excited pair in the conduction band of the QD surrounding – GaAs, "enriched" with interface defects. If there are empty trapping centers, then nonequilibrium electrons rapidly fill them. In the model of spatially indirect optical transitions, the ionization of quantum media with the formation of localized holes is considered as a single process without specification of separate stages. In the case of one trapping level, the photoconduction kinetics is described by the following system of equations:

$$\frac{dp_L}{dt} = g - \beta n p_L, \tag{3}$$

$$\frac{dn_t}{dt} = \gamma(N_t - n_t)n - \omega n_t, \tag{4}$$

$$p_L = n_t + n. \quad (5)$$

Here, g is the hole generation rate in QD, i.e. the number of photoionization acts per unit time, n is the electron concentration in the GaAs conduction band, p_L is the hole concentration in the QD valence band, N_t is the trap concentration, n_t is the concentration of electrons localized in traps, $N_t - n_t$ is the concentration of free traps, γ is the electron trapping coefficient, β is the coefficient of recombination of a free electron with a QD hole, and ω is the probability of thermal activation of an electron — transition from a trap to the conduction band.

The system of equations (3)–(5) is similar to those describing kinetic processes under the impurity-involved excitation of phosphorus with one type of trapping centers [24].

The rise kinetics of the signal is described by the equation:

$$\frac{dn}{dt} \approx g - \beta n(N_t + n). \quad (6)$$

Here, it is taken into account that traps are filled when the photocurrent just starts increasing, i.e. it is negligibly small while electrons are effectively trapped by impurity centers. That is why $n_t \approx N_t$. The solution of Eq.(6) has the following form:

$$n(t) = \sqrt{\frac{g}{\beta} + \frac{N_t^2}{4}} \mathrm{th} \left(t\sqrt{\beta}\sqrt{g + \frac{\beta N_t^2}{4}} \right) - \frac{N_t}{2}. \quad (7)$$

In the stationary case, we have

$$n_{\mathrm{st}} = n(t \to \infty \ \text{ for } \ g \neq 0) = \sqrt{\frac{g}{\beta} + \frac{N_t^2}{4}} - \frac{N_t}{2}. \quad (8)$$

If the excitation is very strong, $n_{\mathrm{st}} \gg N_t$, then $n_{\mathrm{st}} \approx \sqrt{g/\beta}$. We now describe the fall kinetics of the signal under the same conditions, if traps are filled, i.e. $p_L \approx N_t + n$:

$$\frac{dn}{dt} = -\beta n(N_t + n). \quad (9)$$

We obtain a nonlinear differential Bernoulli equation that is reduced to a linear differential equation by the substitution $n = 1/z$. Its solution is presented as

$$n(t) = \frac{1}{(\frac{1}{N_t} + \frac{1}{n_{\mathrm{st}}}) \exp(\beta N_t t) - \frac{1}{N_t}}. \quad (10)$$

At $\beta N_t \ll 1$, one obtains

$$n(t) = \frac{1}{(\frac{1}{N_t} + \frac{1}{n_{\mathrm{st}}}) \beta N_t t + \frac{1}{n_{\mathrm{st}}}}, \quad (11)$$

which corresponds to a first-order hyperbola.

Under the condition $\beta N_t \gg 1$, we derive an exponential attenuation law:

$$n(t) \approx \left(\frac{1}{N_t} + \frac{1}{n_{\mathrm{st}}} \right)^{-1} \exp(-\beta N_t t), \quad (12)$$

It is worth noting that $n(t)$ is the concentration of conduction electrons, which is an additive to the residual concentration existing at large observation times. In other words, it is an additive to $n(t \to \infty)$ after the excitation is switched off.

The derived relations are proved experimentally. For example, the photocurrent presented as a time function of I_{st}/I is described by a straight line at low t (Fig. 4, insets), as is predicted by formula (11).

We did not manage to thoroughly describe the photoconduction kinetics of the $In_{0.5}Ga_{0.5}As$/GaAs samples shown in Fig. 4,*b*. However, it can be qualitatively explained in the following way.

At the beginning, an illuminated sample does not display a photoconduction signal due to the process of filling of the most effective traps. Particularly, the electron trap with $E_c - 165$ meV has a huge capture cross section – 6.5×10^{-14} cm^2 [25]. After the electron saturation, the *S*-like increase of the photocurrent is observed, which is characteristic of photoconductors with trapping centers [26]. Close to $t = 700$ s, one registers a "burst" of the signal – an abrupt increase followed by a relatively flat fall passing into a plateau. Such an anomaly is not specific of classic semiconductors. To our mind, such a behavior can be explained in the following way.

An abrupt growth of the photoconduction takes place after the filling of all interface traps, which results in a fast increase of the free electron concentration. The following fall is a consequence of the drift of free electrons deep into GaAs, where they find new traps, which gives rise to a decrease of the carrier concentration.

4. Conclusions

$In_xGa_{1-x}As$/GaAs heterostructures with QDs at a temperature of 77 K manifest the long-term photocurrent kinetics and the effect of residual conductivity in the absence of exciting radiation. TSC investigations at temperatures lower than 200 K prove the existence of deep local levels in the surrounding of QDs that have properties of electron traps. Analyzing the form of the TSC curve, we obtained the depths of these local trapping levels: $\varepsilon_t = 0.11$ eV, 0.16 eV, 0.21 eV, 0.24 eV, and 0.35 eV. The number of the observed peaks of the TSC curve in the considered structures depended on the location of the Fermi level. In semiinsulating $In_{0.5}Ga_{0.5}As/GaAs$ structures, the Fermi level is located close to the middle of the forbidden band, which allows one to register a wide spectrum of deep states. Using the LPC spectroscopy technique, we have shown that the defect levels lying below the Fermi level are not photoactive. Instead, the electrons from filled levels in the stationary state can be activated under the action of optical excitation and make a contribution to the photocurrent. The LPC spectra also made it possible to reveal the transitions involving levels of electron traps of GaAs intrinsic defects at the InGaAs/GaAs interface, particularly $EL2$ (0.6 eV and 0.75–0.85 eV) and $EB3$ (0.9 eV) ones.

1. M. Grundmann, O. Stier, and D. Bimberg, Phys. Rev. B **52**, 11969 (1995).
2. E.B. Foxman, P.L. McEuen, U. Meirav, N.S. Wingreen, Y. Meir, P.A. Belk, N.R. Belk, M.A. Kastner, and S.J. Wind, Phys. Rev. B **47**, 10020 (1993).
3. Y. Meir, N.S. Wingreen, and P.A. Lee, Phys. Rev. Lett. **66**, 3048 (1991).
4. V.S. Vavilov, P.C. Euthymiou, and G.E. Zardas, Usp. Fiz. Nauk **169**, 209 (1999).
5. M.K. Sheinkman and A.Ya. Shik, Fiz. Tekhn. Polupr. **10**, 209 (1976).
6. L.I. Grossweiner, J. Appl. Phys. **24**, 1306 (1953).
7. D.S. Misra, A. Kumar, and S.C. Agarwal, Phys. Rev. B **31**, 1047 (1985).
8. A.G. Milnes, textitDeep Impurities in Semiconductors (Wiley-Interscience, New York, 1973).
9. O.V. Vakulenko, S D. Kondratenko, S.L. Golovinskii, and I.A. Grin', Visn. Kyiv. Univers. Ser. Fiz. Mat. Nauk. **2**, 247 (2010).
10. T. Asano, Z. Fang, and A. Madhukar, J. Appl. Phys. **107**, 073111 (2010).
11. S.W. Lin, C. Balocco, M. Missous, A.R. Peaker, and A.M. Song, Phys. Rev. B **72**, 165302 (2005).
12. J.S. Kim, E.K. Kim, W.J. Choi, J.D. Song, and J.I. Lee, Jpn. J. Appl. Phys. **45**, 5575 (2006).
13. G.M. Martin, A. Mitonneau, and A. Mircea, Electron. Lett. **13**, 191 (1977).
14. P. Bräunlich, Appl. Phys. Lett. **38**, 2516 (1967).
15. M. Shafi, R.H. Mari, A. Khatab, D. Taylor, and M. Henini, Nanoscale Res. Lett. **5**, 1948 (2010).
16. D.P. Popescu, P.G. Eliseev, A. Stintz, and K.J. Malloy, Semicond. Sci. Technol. **19**, 33 (2004).
17. W.-H. Chang, T.M. Hsu, C.C. Huang, S.L. Hsu, C.Y. Lai, N.T. Yeh, T.E. Nee, and J.-I. Chyi, Phys. Rev. B **62**, 6959 (2000).
18. J.L. Casas Espinola, M. Dybic, S. Ostapenco, T.V. Torchynska, and G. Polupan, J. Phys. Conf. Series **61**, 180 (2006).
19. J. Bloch, J. Shah, L.N. Pfeiffer, K.W. West, and S.N.G. Chu, Appl. Phys. Lett. **77**, 2545 (2000).
20. K. Mukai, N. Ohtsuka, and M. Sugawara, Appl. Phys. Lett. **70**, 2416 (1997).
21. Y.T. Dai, J.C. Fan, Y.F. Chen, R.M. Lin, S.C. Lee, and H.H. Lin, J. Appl. Phys. **82**, 4489 (1997).
22. O.V. Vakulenko and M.P. Lisitsa, *Optical Recharging Recharge of Impurity in Semiconductors* (Naukova Dumka, Kiev, 1992) (in Russian).
23. V.I. Borisov, V.A. Sablikov, I.V. Borisova, and A.I. Chmil', Fiz. Tekhn. Polupr. **33**, 68 (1999).
24. M.V. Fock, *Introduction into Kinetics of Crystal Luminescence* (Nauka, Moscow, 1964) (in Russian).
25. M.M. Sobolev, I.V. Kochnev, V.M. Lantratov, N.A. Bert, N.A. Cherkashin, N.N. Ledentsov, and D.A. Bedarev, Fiz. Tekhn. Polupr. **34**, 200 (2000).
26. R.H. Bube, *Photoconductivity of Solids* (Wiley, New York, 1960).

Received 12.04.11.
Translated from Ukrainian by H.G. Kalyuzhna

ВПЛИВ ДЕФЕКТНИХ СТАНІВ ІНТЕРФЕЙСУ НА ФОТОЕЛЕКТРИЧНІ ВЛАСТИВОСТІ ГЕТЕРОСТРУКТУР $In_xGa_{1-x}As/GaAs$ З КВАНТОВИМИ ТОЧКАМИ

О.В. Вакуленко, С.Л. Головинський, С.В. Кондратенко, Ю.І. Мазур, Ж.М. Ванг, Г.Д. Саламо

Р е з ю м е

У гетероструктурах $In_xGa_{1-x}As/GaAs$ з ланцюгами квантових точок (КТ) з різною концентрацією x індію досліджено властивості латерального фотоструму. При зона-зонному збудженні КТ квантами $h\nu = 1{,}2$ еВ структури виявили довготривалу динаміку наростання та релаксації фотоструму, а також ефект залишкової провідності після вимкнення збуджувального випромінювання. Аналіз даних із термостимульованої провідності (ТСП) після збудження оптичним випромінюванням в області поглинання КТ засвідчив такі значення енергетичних рівнів дефектних станів відносно зони провідності GaAs: 0,11 еВ, 0,16 еВ, 0,21 еВ, 0,24 еВ та 0,35 еВ. На дослідах латеральної фотопровідності (ЛФП) виявлено переходи за участю рівнів електронних пасток власних дефектів у GaAs $EL2$ та $EB3$. У найпростішому випадку наноструктурного фотопровідника з одним центром прилипання для електронів провідності отримано аналітичний вигляд кінетики фотоструму, який підтверджено на дослідах зі зразками $In_{0,4}Ga_{0,6}As/GaAs$. Кінетика фотопровідників $In_{0,5}Ga_{0,5}As/GaAs$ дещо складніша і описана лише якісно.